Journal of Power Sources 196 (2011) 2469–2474

Contents lists available at ScienceDirect

Journal of Power Sources

journal homepage: www.elsevier.com/locate/jpowsour

High activity of Pd–WO_3/C catalyst as anodic catalyst for direct formic acid fuel cell

Ligang Feng, Liang Yan, Zhiming Cui, Changpeng Liu, Wei Xing*

State Key Laboratory of Electroanalytical Chemistry, Changchun Institute of Applied Chemistry, Jilin Province Key Laboratory of Low Carbon Chemical Power, Graduate School of the Chinese Academy of Sciences, 5625 Renmin Street, Changchun, Jilin 130022, PR China

ARTICLE INFO

Article history:
Received 8 November 2010
Accepted 12 November 2010
Available online 19 November 2010

Keywords:
Electrooxidation
Pd nanoparticles
Phosphotungstic acid
Hybrid support
Direct formic acid fuel cell

ABSTRACT

Pd nanoparticles supported on the WO_3/C hybrid are prepared by a two-step procedure and the catalysts are studied for the electrooxidation of formic acid. For the purpose of comparison, phosphotungstic acid (PWA) and sodium tungstate are used as the precursor of WO_3. Both the Pd–WO_3/C catalysts have much higher catalytic activity for the electrooxidation of formic acid than the Pd/C catalyst. The Pd–WO_3/C catalyst prepared from PWA shows the best catalytic activity and stability for formic acid oxidation; it also shows the maximum power density of approximately 7.6 mW cm^{-2} when tested with a small single passive fuel cell. The increase of electrocatalytic activity and stability is ascribed to the interaction between the Pd and WO_3, which promotes the oxidation of formic acid in the direct pathway. The precursors used for the preparation of the WO_3/C hybrid support have a great effect on the performance of the Pd–WO_3/C catalyst. The WO_3/C hybrid support prepared from PWA is beneficial to the dispersion of Pd nanoparticles, and the catalyst has potential application for direct formic acid fuel cell.

1. Introduction

The direct formic acid fuel cell (DFAFC) has received considerable attention due to its several advantages, such as low toxicity, limited fuel crossover and high practical power density [1–4]. Therefore, the research on the catalysts for formic acid oxidation is crucial for the development of DFAFCs. In recent years, the Pd-based catalysts have shown high activity for the electrooxidation of formic acid by overcoming the CO poisoning effect [5–9]. Masel et al. [9,10] reported that Pd and Pd/C catalysts can overcome the CO poisoning and produce high catalytic performances in the DFAFCs. Ha et al. [11–13] investigated the Pd/C catalyst as an anodic catalyst for the DFAFC and indicated that Pd catalysts possess good electrocatalytic activity. The addition of some metals or modifiers such as Co [7], Ir [14], Pb [15], TiO_2 [6] and P [16] to Pd/C catalyst has improved the catalytic activity and stability. However, the activity and stability of the Pd-based catalysts still need further improvements to meet the demand of the DFAFCs.

Tungsten trioxide (WO_3) is an important oxide which has special electrochemical properties for use as an electrocatalyst material. It has been reported that Pt and PtRu catalysts supported on WO_3 had significantly high activity for the electrooxidation of methanol [17–21] and formic acid [22,23]. The results showed that WO_3 had a good assistant electrocatalytic effect with noble metals. It has been elucidated that WO_3 can form a hydrogen bronze (H_xWO_3) which effectively facilitates the dehydrogenation of small organic molecules. To our knowledge, there are few reports on the WO_3/C hybrid used as a catalyst support for the electrooxidation of formic acid. We have reported that the WO_3/C hybrid is a highly active catalyst support for formic acid oxidation [23], which has potential application for DFAFCs. However, both the existent state and the preparation method of WO_3 would affect the final properties of the catalyst. According to the reports [24–26], the PWA was strongly adsorbed onto various active carbons and the adsorbed PWA was not desorbed when washed with hot water or hot methanol. This phenomenon gives us some inspirations. First, the interaction between the PWA and carbon is strong, and the PWA can be uniformly adsorbed onto the carbon surface. Second, the excess PWA could be washed off, but the PWA strongly adsorbed on the carbon surface is still on the carbon surface. Therefore, the well-dispersed WO_3/C support could be obtained by the thermal decomposition of the adsorbed PWA on the carbon surface, and if used as a support, the WO_3/C hybrid support would create a strong interaction between the WO_3 and metal particles.

The objective of this work is to synthesize WO_3/C hybrid as a support for Pd nanoparticles with a novel method and to study the catalytic performances of the catalyst for the electrooxidation of formic acid. Therefore, in this study, the WO_3/C hybrid material was prepared by the thermal decomposition of the adsorbed PWA on carbon, and the corresponding Pd–WO_3/C catalyst (Pd–WO_3/C-A) was prepared by the impregnation reduction method. For comparison, the Pd–WO_3/C-B catalyst was synthesized according to

* Corresponding author. Tel.: +86 431 5262223; fax: +86 431 5685653.
E-mail address: xingwei@ciac.jl.cn (W. Xing).

0378-7753/$ – see front matter © 2010 Elsevier B.V. All rights reserved.
doi:10.1016/j.jpowsour.2010.11.073

the previous work [23], and the Pd/C catalyst was also prepared with the same method. The catalysts were characterized by the X-ray diffraction, transmission electron microscope and energy dispersive X-ray analysis. The electrochemical performances of the catalysts for the electrooxidation of formic acid were studied and the catalysts were also tested as anodic catalyst with a single passive DFAFC in order to further evaluate the catalytic activity.

2. Experimental

2.1. Catalyst preparation

In the first step, the WO_3/C hybrid material was prepared. A given amount of Vulcan XC-72R carbon was added to an aqueous solution of 10 mg mL^{-1} of PWA and maintained at room temperature (20 °C) for 48 h under vigorous agitation. Subsequently, the suspension was filtered and the solid was transferred to a tubular oven at 550 °C for the heat treatment of 6 h to obtain a stable WO_3/C support under the protection of nitrogen.

In the second step, the Pd–WO_3/C-A catalyst was synthesized. First, a given amount of the above WO_3/C hybrid material was ultrasonically dispersed in 50 mL of deionized water and second, an appropriate amount of H_2PdCl_4 solution was added to the suspension under agitation. After thoroughly mixing, the pH value of the suspension was adjusted to ca. 7 with a 5% NaOH solution. It was stirred for half an hour before an excess of freshly prepared $NaBH_4$ solution was added dropwise into the above mixture in the PH range 7–9. Subsequently, an additional 4 h of stirring was performed to complete the reaction. Finally, the suspension was filtered, washed and dried overnight at 80 °C in a vacuum oven.

The Pd–WO_3/C-B catalyst (WO_3 content 20 wt%, the best one) was synthesized using sodium tungstate as the precursor of WO_3 [23]. The Pd/C catalyst was also prepared with the above method. The nominal content of Pd in the catalysts was 20 wt%. All solutions were prepared using Millipore-Milli Q water and analytical-grade reagents.

2.2. Catalyst characterization

The X-ray diffraction (XRD) patterns were obtained using a Rigaku-D/MAX-PC 2500 X-ray diffractometer with Cu Kα (λ = 1.5405 Å) as a radiation source operating at 40 kV and 200 mA. The composition of the catalysts was measured by energy dispersive X-ray analysis (EDX) with a JEOL JAX-840 scanning electron microscope operating at 20 kV. The transmission electron microscope (TEM) images were obtained by using a JEOL 2010 microscope operating at 200 kV with nominal resolution. The catalyst samples were prepared by dispersing the catalyst/ethanol suspension onto a 3 mm diameter copper grid covered with carbon film and then evaporating the solvent in air.

2.3. Electrochemical measurements

Electrochemical measurements were performed with an EG&G Par potentiostat/galvanostat (Model 273A, Princeton Applied

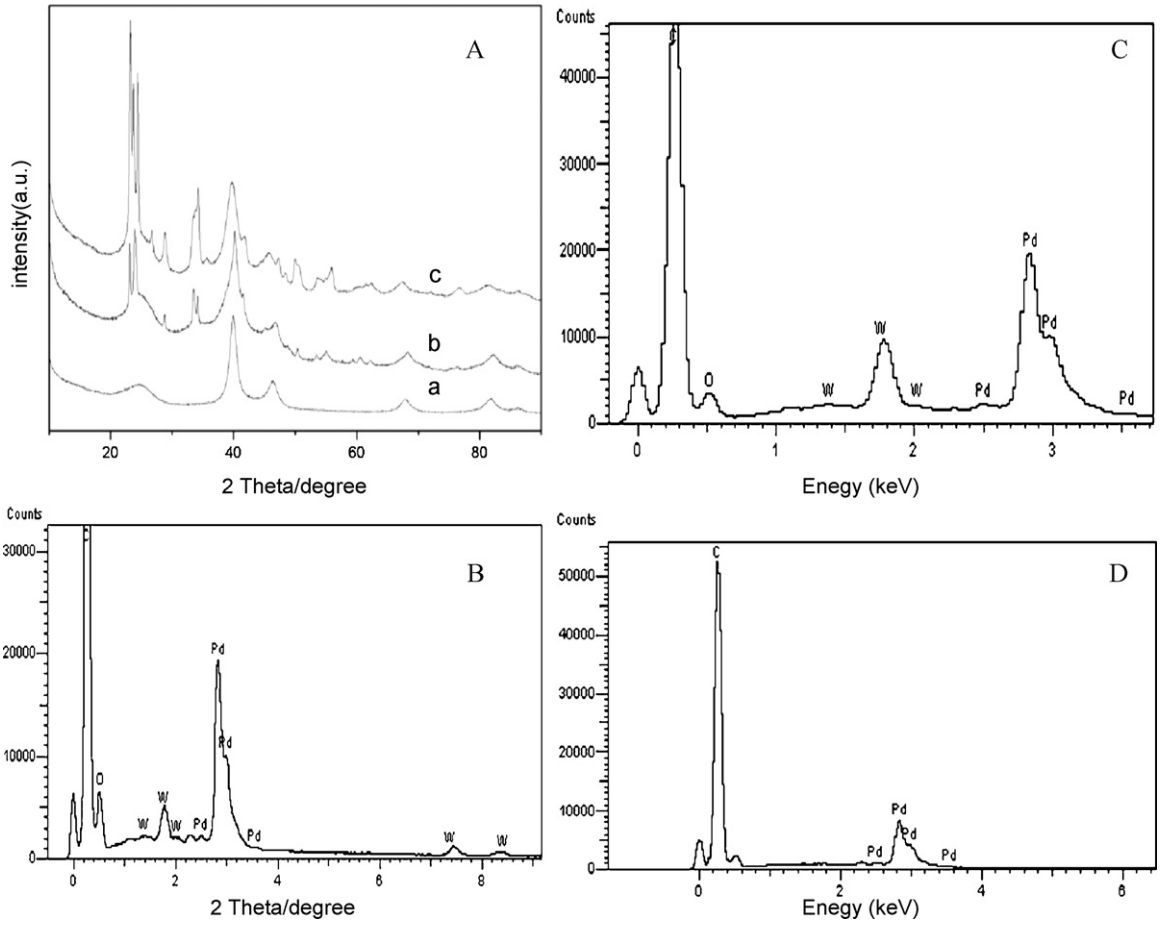

Fig. 1. XRD patterns of the Pd/C (a), Pd–WO_3/C-A (b) and Pd–WO_3/C-B (c) catalyst (A). EDX spectrum of the Pd–WO_3/C-A catalyst (B), Pd–WO_3/C-B catalyst (C) and Pd/C catalyst (D).

Research Co. USA) and a conventional three-compartment electrochemical cell. A Pt plate and an Ag/AgCl electrode were used as the counter electrode and reference electrode, respectively. All potentials were quoted against the Ag/AgCl electrode. The working electrode was prepared as follows. First, 5 mg of the catalyst was dispersed ultrasonically in 1 mL of the alcohol solution containing 50 μL Nafion solution (5 wt%, Aldrich Co. USA). Second, 10 μL of the above solution was pipetted and spread on a mirror-finished glassy carbon electrode with 3 mm diameter. At last, it was dried at room temperature for 30 min. The glassy carbon electrode was polished with alumina slurry of 0.5 and 0.03 μm successively before use. The apparent surface area of the glassy carbon electrode was 0.07 cm^2.

All electrochemical measurements were carried out in a 0.5 M H_2SO_4 solution with or without 0.5 M HCOOH deaerated by pure nitrogen for 15 min prior to any measurements. For the electrooxidation of formic acid, the potential range was from −0.2 to +0.8 V. The CO_{ad} stripping voltammograms were measured in a 0.5 M H_2SO_4 solution. CO was purged into the 0.5 M H_2SO_4 solution for 15 min to allow the complete adsorption of CO onto the catalyst when the working electrode was kept at 0 mV vs. Ag/AgCl electrode, and excess CO in the electrolyte was purged out with N_2 for 15 min. The amount of CO_{ad} was evaluated by integration of the CO_{ad} stripping peak. All the measurements were carried out at room temperature and the stable results were reported.

In order to further evaluate the properties of the catalyst, the catalyst was tested as anodic catalyst with a small home-made single passive DFAFC [3,27]. Pt black (Johnson Matthey) and the home-made catalysts both with 4 mg cm^{-2} were used as the cathodic and anodic catalysts, respectively. The membrane electrode assemble (MEA), active area of 4 cm^2, was fabricated by hot pressing the anodic and cathodic electrode onto two sides of the Nafion 117 membrane at 130 °C and 3.5 MPa for 3 min. The performance of the cell was measured with a Fuel Cell Test System (Arbin Instruments Co.) at ambient conditions with 3.0 M formic acid solution.

3. Results and discussion

Fig. 1A shows XRD patterns of the Pd–WO_3/C-A, Pd–WO_3/C-B and Pd/C catalysts. The diffraction peaks at ca. 39, 46, 68 and 81° observed in the three catalysts corresponded to the face-centered cubic phase (fcc) of Pd, while other peaks at ca. 22, 24, 34, 50, 53, 55 and 61° observed in the Pd–WO_3/C-A (curve b) and Pd–WO_3/C-B (curve c) catalyst corresponded to the monoclinic phase of WO_3 [28,29]. The diffraction peak at ca. 25° observed in the Pd/C catalyst (curve a) corresponded to the (0 0 2) plane reflection of Vulcan XC-72 carbon, while the diffraction peaks at ca. 25° in the Pd–WO_3/C-A (curve b) and Pd–WO_3/C-B (curve c) catalysts were assigned to the mixture of the (0 0 2) reflection of Vulcan XC-72 carbon and (0 2 0) reflection of WO_3. A separated fcc phase of Pd and a monoclinic

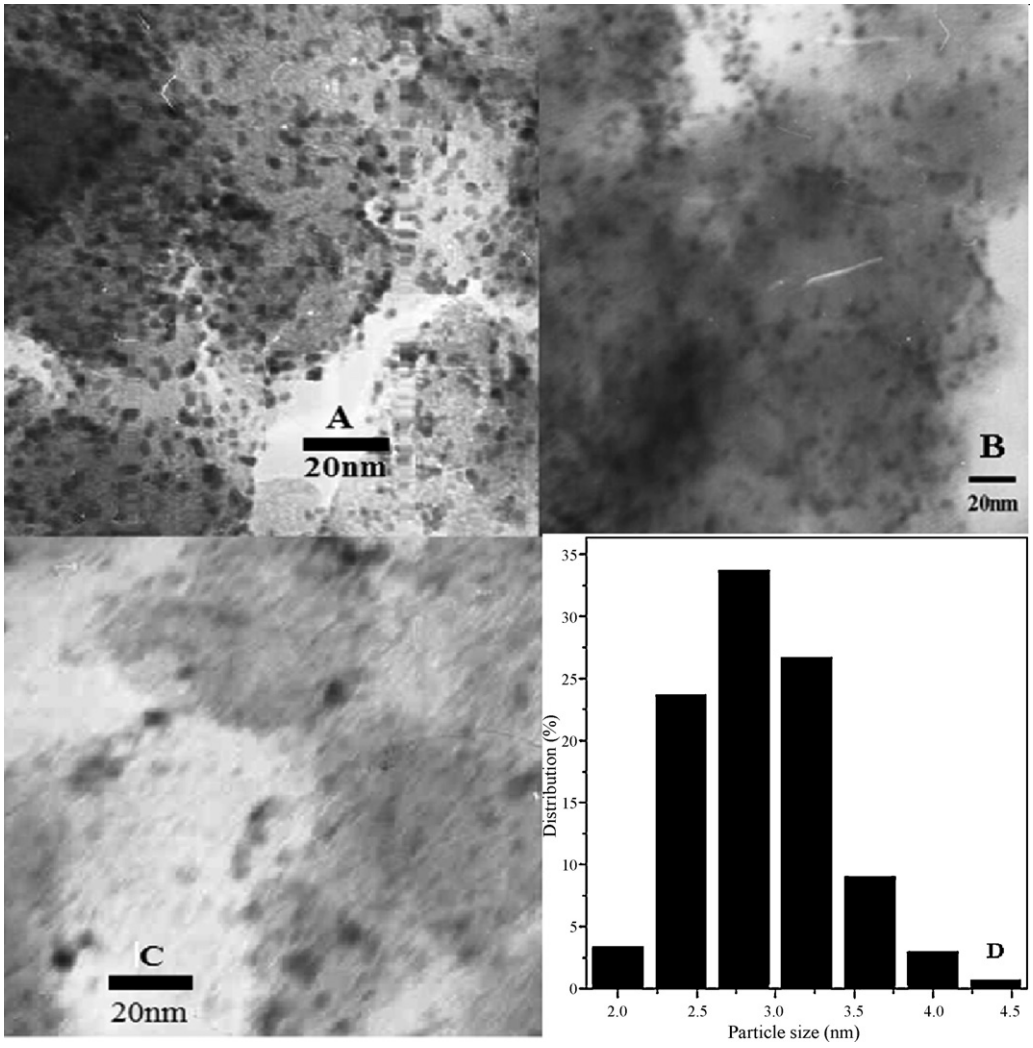

Fig. 2. TEM images of Pd–WO_3/C-A (A), Pd–WO_3/C-B (B), Pd/C (C) catalyst and the size distribution histogram of the Pd–WO_3/C-A catalyst.

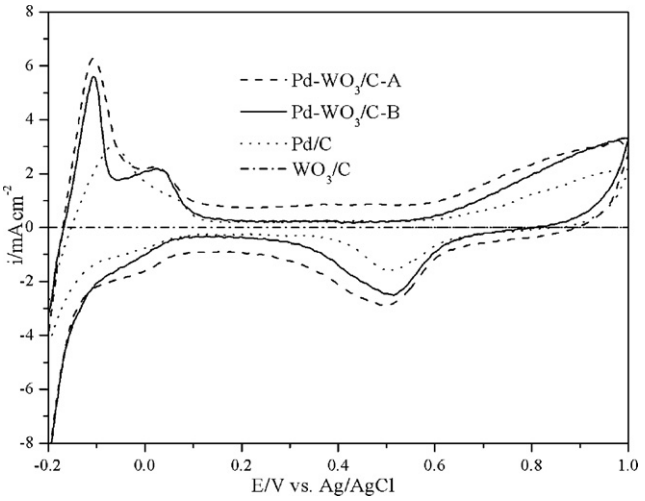

Fig. 3. Cyclic voltammograms of the Pd–WO_3/C-A, Pd–WO_3/C-B, Pd/C catalyst and WO_3/C support in a 0.5 M H_2SO_4 solution at a scan rate of 50 mV s^{-1}.

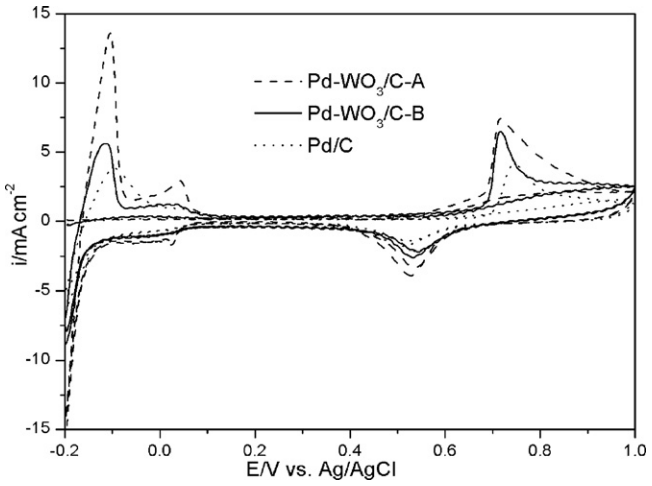

Fig. 4. CO_{ad} stripping voltammograms of the Pd–WO_3/C-A, Pd–WO_3/C-B and Pd/C catalyst in a 0.5 M H_2SO_4 solution at a scan rate of 20 mV s^{-1}.

phase of WO_3 can be observed from the characteristic peaks of Pd and WO_3 in the Pd–WO_3/C catalysts. Compared to Pd/C (a) and Pd–WO_3/C-B(c) catalysts, the characteristic peaks of Pd–WO_3/C-A (b) shifted remarkably towards the higher direction of 2θ values, indicating the formation of an alloy phase in the Pd–WO_3/C-A catalyst. The EDX spectrum of the Pd–WO_3/C-A, Pd–WO_3/C-B and Pd/C catalyst is shown in Fig. 1B, C and D, respectively. The weight percentages of Pd and WO_3 in the Pd–WO_3/C-A catalyst were 21.17% and 8.05%, respectively. The weight percentages of Pd and WO_3 in the Pd–WO_3/C-B catalyst were 20.96% and 18.75%, respectively. The weight percentage of Pd in the Pd/C catalyst was 20.67%. Other trace elements like Cl and P were not found.

Fig. 2 shows the TEM images of the Pd–WO_3/C-A (A), Pd–WO_3/C-B (B) and Pd/C (C) catalysts. The Pd nanoparticle sizes in the Pd/C (C) catalyst were primarily distributed within the range of 3–5 nm, but some of the Pd nanoparticles were severely aggregated. The Pd nanoparticles on the WO_3/C hybrid support for the Pd–WO_3/C-A and Pd–WO_3/C-B catalysts had a remarkably uniform and rather narrow size distribution. The distribution of the metal particles in the Pd–WO_3/C-A catalyst was obtained by measuring 300 particles randomly and the corresponding histogram of the size distribution is shown in Fig. 2D, indicating that the average particle size of Pd was approximately 3 nm. The average particle size of the Pd for the Pd–WO_3/C-B catalyst was approximately 3.5 nm.

Fig. 3 shows the cyclic voltammograms (CVs) of the Pd–WO_3/C-A, Pd–WO_3/C-B, Pd/C catalysts and the WO_3/C support in 0.5 M H_2SO_4 solution. Compared to the three Pd catalysts, the oxidation current of the WO_3/C support was negligible. According to the area of the hydrogen adsorption/desorption peaks of the three catalysts, both the Pd–WO_3/C-A and Pd–WO_3/C-B catalysts had a larger peak area than the Pd/C catalyst, which indicated that they possessed a larger electrochemical surface area (ESA). Furthermore, the potential values of the hydrogen desorption peaks for the Pd–WO_3/C-A and Pd–WO_3/C-B catalysts were close to each other. Compared to the Pd/C catalyst, the peak potentials of both Pd–WO_3/C catalysts shifted towards a negative direction, indicating that the adsorption strength of hydrogen on the Pd surface was weakened, which can be attributed to the hydrogen spillover effect of WO_3 [23,30]. Here, the CO_{ad} stripping method was used to evaluate the EAS quantitatively. Fig. 4 shows the CO_{ad} stripping voltammograms for the three catalysts in a 0.5 M H_2SO_4 solution. There was a well-defined stripping peak of CO_{ad} at the potential of approximately 0.71 V for both Pd–WO_3/C catalysts and 0.75 V for the Pd/C catalyst, respectively. Compared to the Pd/C catalyst, the onset and the peak potentials for CO_{ad} oxidation on both Pd–WO_3/C catalysts were shifted negatively, which was an indication that the addition of WO_3 was helpful in weakening the CO adsorptive bond on the Pd active sites. It was evident that the stripping peak area at the Pd–WO_3/C-A catalyst was much larger than that of the Pd–WO_3/C-B and the Pd/C catalyst, indicating that there were much more active surface sites on the Pd–WO_3/C-A catalyst. Furthermore, the ESA for the catalyst was calculated by using the CO_{ad} oxidation charge after subtracting the background current. It was 21.1, 13.1, and 9.4 m^2 g^{-1} for the Pd–WO_3/C-A, Pd–WO_3/C-B, and Pd/C catalysts, respectively. The ESA of the catalyst was ordered as Pd–WO_3/C-A > Pd–WO_3/C-B > Pd/C catalyst. This result was consistent with those obtained by the hydrogen stripping method and the physical characterization. Specifically for the Pd–WO_3/C-A catalyst, the ESA was enhanced by a factor of 2.2 as compared to Pd/C catalyst, which meant that the addition of WO_3 had a promotion effect on the stripping removal of the CO molecules adsorbed on the Pd surface.

Fig. 5 displays the CVs for the electrooxidation of formic acid in a 0.5 M H_2SO_4 solution containing 0.5 M formic acid on the three catalysts and the WO_3/C support with a sweep rate of 20 mV s^{-1}. It was evident that the WO_3/C support had almost no catalytic activity for

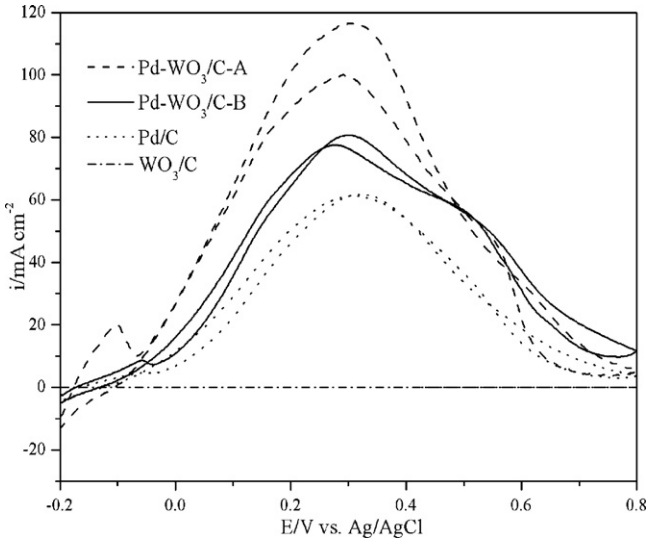

Fig. 5. Cyclic voltammograms for the electrooxidation of formic acid in a 0.5 M H_2SO_4 solution containing 0.5 M formic acid for the Pd–WO_3/C-A, Pd–WO_3/C-B, Pd/C catalyst and WO_3/C support at a scan rate of 20 mV s^{-1}.

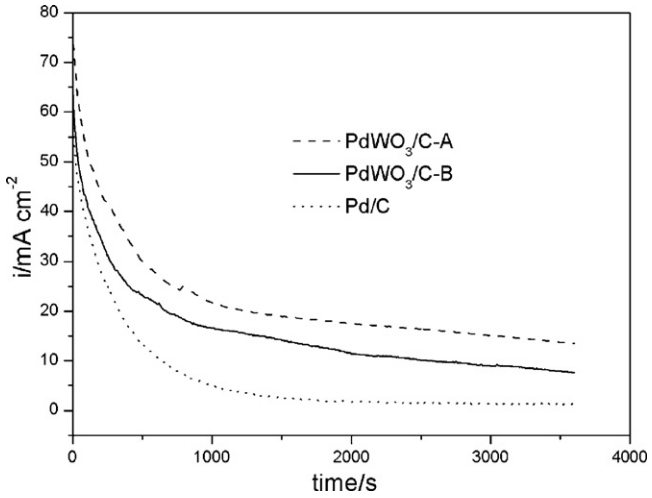

Fig. 6. Chronoamperometric curves for the Pd–WO_3/C-A, Pd–WO_3/C-B and Pd/C catalyst at 0.2 V in a 0.5 M H_2SO_4 solution containing 0.5 M formic acid.

formic acid oxidation. According to the oxidation current, the electrooxidation activity of the catalysts for formic acid was ordered as Pd–WO_3/C-A > Pd–WO_3/C-B > Pd/C catalyst. The peak current of Pd–WO_3/C-A catalyst was 1.9 times as large as that of the Pd/C catalyst and 1.4 times as large as that of Pd–WO_3/C-B catalyst. The order of the electrooxidation activity was consistent with the order of ESA. The potential of the main peak for the electrooxidation of formic acid at both the Pd–WO_3/C catalysts was negatively shifted approximately 30 mV in the positive scan direction, which indicated a promotion effect of WO_3 in the Pd–WO_3/C catalysts.

Fig. 6 shows the chronoamperometric curves of the three catalysts at 0.2 V in a 0.5 M H_2SO_4 solution containing 0.5 M formic acid. The currents at the Pd–WO_3/C-A, Pd–WO_3/C-B and Pd/C catalysts at 3600 s were 13.5, 7.6 and 1.4 mA cm^{-2}, respectively. The stability of the catalysts was ordered as Pd–WO_3/C-A > Pd–WO_3/C-B > Pd/C catalyst, which was also consistent with the above results. Therefore, the results further demonstrated that the addition of WO_3 can greatly improve the activity and stability of the catalyst for the electrooxidation of formic acid.

The polarization and power density curves of a single passive DFAFC with the three catalysts as anode are shown in Fig. 7. It was evident that the Pd–WO_3/C-A catalyst had the best performance. The maximum power density was approximately 7.6, 6.0 and 4.2 mW cm^{-2} for Pd–WO_3/C-A, Pd–WO_3/C-B and Pd/C catalyst,

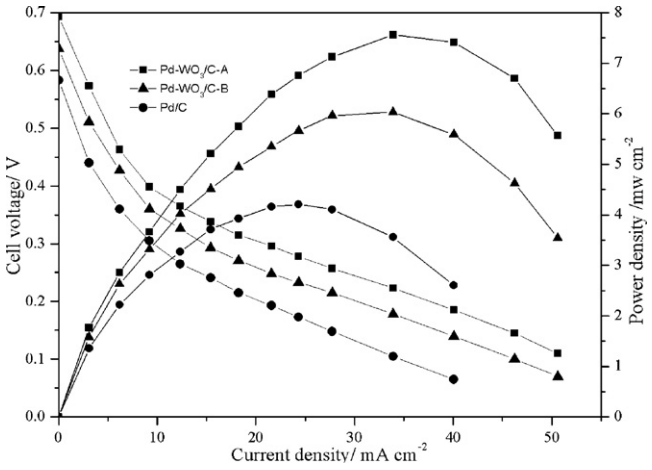

Fig. 7. Polarization and power density curves of a single passive DFAFC with Pd–WO_3/C-A, Pd–WO_3/C-B and Pd/C catalyst as anodic catalyst.

respectively. This was a preliminary result and the performance was not high for DFAFC which may be due to the low catalyst loading and not optimized MEA preparation method. However, it was evident that this result confirmed the advantage of adding WO_3 into Pd catalysts for formic acid oxidation. According to this result, the activity of Pd–WO_3/C-A catalyst had increased by approximately 20% and 45% as compared to the Pd–WO_3/C-B and Pd/C catalyst.

It has been accepted that the electrooxidation of formic acid on the Pd/C catalyst is primarily through the direct dehydrogenation way [5–9]. Therefore, a large quantity of hydrogen could adsorb onto the surface of Pd during the electrooxidation of formic acid, and the adsorbed hydrogen could occupy many Pd active sites which hindered the adsorption of formic acid molecules. Because the WO_3 could form bronzes, the adsorbed hydrogen on Pd surface could spill over onto the WO_3 surface [17,20], and then the Pd active sites occupied by the hydrogen atoms were released and could absorb the formic acid molecules. The above process was repeated, which can accelerate the electrooxidation of formic acid. In addition, according to Yoshiike and Kondo [31,32], the water molecules were not only physisorbed but also chemisorbed on the surface of WO_3. The oxophilic nature of WO_3 can promote the adsorption and transformation of the intermediates. Therefore, the catalytic process on the surface of Pd can go on, thereby favoring the electrooxidation of formic acid by the direct dehydrogenation pathway.

The performances of both Pd–WO_3/C-A and Pd–WO_3/C-B catalysts were much better than those of Pd/C catalyst. However, it was interesting that the Pd–WO_3/C-A catalyst with low content of WO_3 had much better catalytic activity and stability than the Pd–WO_3/C-B catalyst. The promotion effect should come from the interaction between Pd and WO_3. Therefore, the WO_3 only intimately contacted with the Pd nanoparticles was more effective in the promotion effect on the electrooxidation of formic acid. Because of the poor conductivity of WO_3, the high WO_3 content in the catalyst would cause the drop of the support conductivity, thereby leading to the low catalytic activity. The reason may be attributed to the different preparation of the WO_3/C support. The WO_3/C support in the Pd–WO_3/C-B catalyst was obtained using Na_2WO_4 as the precursor. During the preparation process, sodium tungstate was transformed to the colloid tungstenic acid coated on the carbon surface, but the coated layer was not uniform and some colloid was not deposited onto the carbon surface. Therefore, the prepared WO_3/C dropped the catalyst conductivity. However, the WO_3/C support in the Pd–WO_3/C-A catalyst was prepared from the PWA which was self-adsorbed on the carbon surface by the strong adsorptive action. The excess PWA and the PWA without strong adsorption on carbon surface were washed off. Therefore, the prepared WO_3 was well dispersed on the carbon surface. When the Pd was reduced, the Pd nanoparticles formed on the anchor sites of WO_3 and it did not largely drop the catalyst conductivity. Therefore, it was evident that the Pd–WO_3/C-A catalyst had much higher catalytic activity for the electrooxidation of formic acid.

4. Conclusion

This study demonstrated that Pd nanoparticles supported on WO_3/C hybrid had significantly enhanced the electrocatalytic performances for the formic acid oxidation. The Pd nanoparticles in the Pd–WO_3/C-A catalyst had a uniform and narrow size distribution from TEM characterization. The ESA obtained by CO_{ad} stripping method was ordered as Pd–WO_3/C-A > Pd–WO_3/C-B > Pd/C catalyst. The CVs measurements showed that the activity of the Pd–WO_3/C-A catalyst for the electrooxidation of formic acid was 1.9 times as large as that of the Pd/C catalyst and 1.4 times as large as that of the Pd–WO_3/C-B catalyst. The catalytic stability was also

ordered as Pd–WO_3/C-A > Pd–WO_3/C-B > Pd/C catalyst, which was consistent with the order of the ESA and the catalytic activity. The maximum power density increased by approximately 20% and 45% as compared to Pd–WO_3/C-B and Pd/C catalysts. The results also indicated that the preparation methods of WO_3/C hybrid support had a great effect on the performances of Pd–WO_3/C catalyst. The WO_3/C hybrid support obtained using PWA as the precursor was beneficial to the dispersion of Pd nanoparticles and most of WO_3 in the catalyst could intimately contact with Pd nanoparticles, which caused the Pd–WO_3/C-A catalyst to have the best performance for the electrooxidation of formic acid.

Acknowledgements

This work was supported by the High Technology Research Program (863 program 2007AA05Z159, 2007AA05Z143) of the Science and Technology Ministry of China and the National Natural Science Foundation of China (20933004, 21011130027 and 21073180).

References

[1] Y.M. Zhu, S.Y. Ha, R.I. Masel, J. Power Sources 130 (2004) 8–14.
[2] X.W. Yu, P.G. Pickup, J. Power Sources 182 (2008) 124–132.
[3] S. Ha, B. Adams, R.I. Masel, J. Power Sources 128 (2004) 119–124.
[4] Y.W. Rhee, S.Y. Ha, R.I. Masel, J. Power Sources 117 (2003) 35–38.
[5] H.Q. Li, G.Q. Sun, Q. Jiang, M.Y. Zhu, S.G. Sun, Q. Xin, J. Power Sources 172 (2007) 641–649.
[6] W.F. Xu, Y. Gao, T.H. Lu, Y.W. Tang, B. Wu, Catal. Lett. 130 (2009) 312–317.
[7] X.M. Wang, Y.Y. Xia, Electrochem. Commun. 10 (2008) 1644–1646.
[8] J.L. Haan, R.I. Masel, Electrochim. Acta 54 (2009) 4073–4078.
[9] R. Larsen, S. Ha, J. Zakzeski, R.I. Masel, J. Power Sources 157 (2006) 78–84.
[10] Y.M. Zhu, Z. Khan, R.I. Masel, J. Power Sources 139 (2005) 15–20.
[11] Z.L. Liu, X.H. Zhang, L. Hong, Electrochem. Commun. 11 (2009) 925–928.
[12] S. Ha, R. Larsen, R.I. Masel, J. Power Sources 144 (2005) 28–34.
[13] W.S. Jung, J. Han, S. Ha, J. Power Sources 173 (2007) 53–59.
[14] X. Wang, Y. Tang, Y. Gao, T.H. Lu, J. Power Sources 175 (2008) 784–788.
[15] X.W. Yu, P.G. Pickup, J. Power Sources 192 (2009) 279–284.
[16] L.L. Zhang, Y.W. Tang, J.C. Bao, T.H. Lu, C. Li, J. Power Sources 162 (2006) 177–179.
[17] S. Jayaraman, T.F. Jaramillo, S.H. Baeck, E.W. McFarland, J. Phys. Chem. B 109 (2005) 22958–22966.
[18] K.W. Park, J.H. Choi, K.S. Ahn, Y.E. Sung, J. Phys. Chem. B 108 (2004) 5989–5994.
[19] J. Rajeswari, B. Viswanathan, T.K. Varadarajan, Mater. Chem. Phys. 106 (2007) 168–174.
[20] T. Maiyalagan, B. Viswanathan, J. Power Sources 175 (2008) 789–793.
[21] P.K. Shen, A.C.C. Tseung, J. Electrochem. Soc. 141 (1994) 3082–3090.
[22] K.Y. Chen, P.K. Shen, A.C.C. Tseung, J. Electrochem. Soc. 142 (1995) L54–L56.
[23] Z.H. Zhang, Y.J. Huang, J.J. Ge, C.P. Liu, T.H. Lu, W. Xing, Electrochem. Commun. 10 (2008) 1113–1116.
[24] Y. Izumi, K. Urabe, Chem. Lett. 5 (1981) 663–666.
[25] M.A. Schwegler, P. Vinke, M. van der Eijk, H. van Bekkum, Appl. Catal. A: Gen. 80 (1992) 41–57.
[26] P.J. Kulesza, M. Chojak, K. Karnicka, K. Miecznikowski, B. Palys, A. Lewera, A. Wieckowski, Chem. Mater. 16 (2004) 4128–4134.
[27] P. Hong, S. Liao, J. Zeng, X. Huang, J. Power Sources 195 (2010) 7332–7337.
[28] P. Trogadas, V. Ramani, J. Electrochem. Soc. 155 (2008) B696–B703.
[29] X. Cui, J. Shi, H. Chen, L. Zhang, L. Guo, J. Gao, J. Li, J. Phys. Chem. B 112 (2008) 12024–12031.
[30] B.S. Hobbs, A.C.C. Tseung, Nature 222 (1969) 556–558.
[31] N. Yoshiike, S. Kondo, J. Electrochem. Soc. 130 (1983) 2283–2287.
[32] N. Yoshiike, S. Kondo, J. Electrochem. Soc. 131 (1984) 809–812.